Quantal properties of spontaneous EPSCs in neurones of the guinea-pig dorsal lateral geniculate nucleus

Ole Paulsen *† and Paul Heggelund *‡

*Department of Neurophysiology, University of Oslo, PO Box 1104 Blindern, N-0317 Oslo, Norway and †University Department of Pharmacology, Mansfield Road, Oxford OX1 3QT, UK

1. Spontaneous non-NMDA glutamate receptor-mediated EPSCs were recorded with the whole-cell patch-clamp technique from twenty-six neurones in the dorsal lateral geniculate nucleus in thalamic slices from guinea-pig.

2. Amplitude distributions of the EPSCs were skewed towards larger values. The skewness could be accounted for by multiquantal properties. The multiquantal properties were most clearly demonstrated in four cells that had prominent peaks in the amplitude distribution, and peak separation approximately corresponding to the modal value. The amplitude distribution for all cells could be adequately fitted by a quantal model consisting of a sum of Gaussians with means equal to integer multiples of a quantal unit. The variance of each Gaussian was equal to the sum of the noise variance of the recordings and an additional non-negative variance which increased linearly with the number of the Gaussian in the series. The estimated mean quantal size was 152 ± 37 pS. The estimated mean quantal coefficient of variation was 15%. Addition of tetrodotoxin did not significantly change any of the quantal parameters ($n = 5$).

3. The waveform of the EPSCs was similar for small and large events, and similar to that of events evoked by stimulation of retinal input fibres. There was a positive correlation between peak amplitude and rise time. This is the opposite of that expected if differences in electrotonic distances were to explain differences in amplitude.

4. The spontaneous EPSCs occurred randomly at an average frequency of 3·1 Hz. The events with amplitudes approximately equal to multiples of the quantal size were, in most cells, more numerous than could be accounted for by coincidence of randomly occurring events of quantal size.

5. The results indicate that spontaneous EPSCs can reflect more than a single quantum, and suggest that quantal events may be coupled due to action potential-independent near-synchronous multiquantal release of transmitter.

Excitatory postsynaptic currents (EPSCs) in central neurones evoked by stimulation of single input fibres may fluctuate in steps of unit size (Redman, 1990; Kullmann & Nicoll, 1992; Stern, Edwards & Sakmann, 1992; Jonas, Major & Sakmann, 1993; Paulsen & Heggelund, 1994). The steps are often reflected in multimodal amplitude distributions with equidistant peaks (Kullmann & Nicoll, 1992; Stern *et al.* 1992; Jonas *et al.* 1993; Paulsen & Heggelund, 1994). Such stepwise fluctuations are often regarded as evidence for quantal release of transmitter substance (Jack, Redman & Wong, 1981) in line with the interpretation of the classical data from the neuromuscular junction (del Castillo & Katz, 1954). Synaptic events may also occur spontaneously. Spontaneous events that occur when action potentials are blocked by tetrodotoxin, miniature events, are assumed to be caused by release of a single quantum (del Castillo & Katz, 1954). Thus, an obvious measure of the quantal size is the magnitude of the miniature event (Van der Kloot, 1991). At the neuromuscular junction the amplitude distribution of miniature events was normally distributed around a mean that corresponded to the unit step in the evoked events (Fatt & Katz, 1952; Boyd & Martin, 1956). This correspondence was essential for the proposal of the quantal nature of synaptic transmission (del Castillo & Katz, 1954). In central excitatory synapses it has been difficult to establish a similar correspondence between steps in evoked events and amplitudes of

‡ To whom correspondence should be addressed.

miniature events. The amplitude distribution of miniature events usually deviates from a normal distribution and is typically skewed towards larger events comprising a broad range of amplitudes (Bekkers, Richerson & Stevens, 1990; Raastad, Storm & Andersen, 1992; Silver, Traynelis & Cull-Candy, 1992; Jonas *et al.* 1993). For excitatory synapses in the hippocampus, this skewness has been attributed to fluctuations in the quantal size at each synaptic site (Bekkers *et al.* 1990; Raastad *et al.* 1992). A large variability of the quantal size with a coefficient of variation in excess of 50% was found in some studies (Bekkers *et al.* 1990). Such large variability is inconsistent with estimates of quantal parameters from evoked excitatory events. Amplitude distributions of evoked events indicate small to moderate quantal variance (Redman, 1990; Larkman, Stratford & Jack, 1991; Kullmann & Nicoll, 1992; Liao, Jones & Malinow, 1992; Jonas *et al.* 1993).

The dorsal lateral geniculate nucleus (dLGN) is a useful preparation for studies of quantal mechanisms. The dLGN cells are electrotonically compact (Bloomfield, Hamos & Sherman, 1987; Crunelli, Leresche & Parnavelas, 1987), and retinogeniculate synapses are concentrated in the proximal region of the dendritic arbor (Wilson, Friedlander & Sherman, 1984; Hamos, Van Horn, Raczkowski & Sherman, 1987; Robson, 1993). In a previous study (Paulsen & Heggelund, 1994) we analysed quantal properties of EPSCs in dLGN cells evoked by stimulation of putative single afferent fibres in the optic tract in thalamic slices. We demonstrated a correspondence of the quantal size for evoked and spontaneous events as seen in the neuromuscular junction. In low extracellular calcium, amplitude distributions of evoked EPSCs had equidistant peaks, and the equidistance corresponded approximately to the modal value of the amplitude distribution of spontaneous EPSCs. The amplitude distribution of the spontaneous EPSCs was skewed towards larger events as in previous studies, but the distribution was multimodal with equidistant peaks, similar to that reported for central inhibitory synapses (Edwards, Konnerth & Sakmann, 1990; Ropert, Miles & Korn, 1990). The broad and skewed amplitude distributions may therefore reflect a quantal distribution of spontaneous events rather than a broad variability in the quantal size.

To test this hypothesis, in the present study we analysed quantal properties of fast spontaneous EPSCs in dLGN cells presumably arising from retinogeniculate synapses. The results were consistent with the hypothesis that the spontaneous EPSCs were quantized. The amplitude distributions of the spontaneous EPSCs were skewed as in previous studies, but the skewness could be accounted for by multiquantal events. These putative multiquantal spontaneous events could not be accounted for by summation of randomly occurring single quanta. The same result was obtained in tetrodotoxin. These results suggest that coupled release of quanta may occur independently of pre-synaptic tetrodotoxin-sensitive action potentials.

METHODS

Adult guinea-pigs (200–350 g) were deeply anaesthetized with halothane and decapitated. The skull was opened and a vertical cut was made through each hemisphere of the brain at the level of the bregma ~30 deg on the frontal plane. The cut plane was fixed with cyanoacrylate glue onto the stage of a vibraslice after removing and chilling a block of the brain including the thalamus in a solution at ~4 °C containing (mM): sucrose, 248; KCl, 2; KH_2PO_4, 1·25; $MgSO_4$, 2; $CaCl_2$, 2; $NaHCO_3$, 26; and glucose, 12 (pH 7·4, equilibrated with 95% O_2 and 5% CO_2). Slices (400 μm thick) were cut through the dLGN and stored at room temperature (20–25 °C) for 2–12 h in an interface-type of incubation chamber. The perfusion solution in the chamber was the same as described above except that 124 mM NaCl replaced the sucrose. Slices were transferred one by one to a submerged-type recording chamber. The recording chamber was perfused at a rate of 2–3 ml min^{-1} with the same type of solution as used during the storage of slices. The superfusion fluid had a temperature of 26–28 °C. To block fast inhibitory postsynaptic currents (IPSCs) 20 μM (−)-bicuculline methochloride or 100 μM picrotoxin was added to the superfusion medium. *N*-Methyl-D-aspartate (NMDA) receptors were blocked with 50 μM DL-2-amino-5-phosphonovaleric acid (APV). All drugs were added to the superfusion fluid by dilution of 1000:1 stock solutions.

Whole-cell recordings were made following the 'blind' patching procedure (Blanton, Lo Turco & Kriegstein, 1989) with a patch-clamp amplifier (Axopatch-1C; Axon Instruments) in the voltage-clamp mode at holding potentials between −55 and −75 mV. The patch pipettes, made from borosilicate glass tubing (Hilgenberg, Malsfeld, Germany), were filled with a solution containing (mM): CsCl, 140; Mg-ATP, 2; GTP, 0·3; EGTA, 0·2; and Hepes, 10 (titrated with NaOH to pH 7·2); they had a resistance of 3–5 MΩ. No correction was made for liquid junction potentials and no compensation was made for electrode resistance. The signals were filtered at 2 kHz (Bessel filter of Axopatch-1C), and digitized at 48 kHz for storage on digital audio tape.

All data analyses were made off-line by computer. Data from stable recording epochs were fed into the computer at an A/D conversion rate of 10 kHz. Spontaneous EPSCs were identified by their similarity in shape to EPSCs evoked by electrical stimulation in the optic tract (Paulsen & Heggelund, 1994). The amplitude of each single event was measured by manual positioning of a vertical cursor on the start and on the peak of the EPSC trace presented on a computer display. The actual amplitude of the event was unknown during this measurement because of automatic amplitude scaling of the trace on the display. Rise time was measured as the time between 20 and 80% of the peak amplitude. Fall time was defined as the time of decay from the peak amplitude to 50% of the peak amplitude. The computer program generated a horizontal cursor at the level of 50% of peak amplitude, and the magnitude of the fall time was measured by manual positioning of a vertical cursor at the intersection between the current trace and the horizontal cursor. Background noise was determined from two automatic measurements taken before each EPSC. In each of the two measurements the amplitude difference was determined between two points separated in time by the same interval as the interval between the start and the peak of the subsequent EPSC. The two noise measurements started 4 and 1 ms before the start of the EPSC. Baseline periods contaminated by other spontaneous EPSCs were excluded from the noise estimates. Estimated quantal sizes are given in conductance changes in order to facilitate the

comparison between experiments. The conductance changes were estimated by assuming a reversal potential for the EPSC of ~0 mV.

Amplitude frequency histograms made for each cell were first inspected for the presence of peaks to obtain a pre-estimate of quantal size. A sum of Gaussian distributions was fitted to the data by maximum likelihood estimation using the expectation–maximization algorithm on finely binned data (0·3 pA; Kullmann, 1989). The Gaussians were separated by equal increments. A Kolmogorov–Smirnov test (K–S test) was used to evaluate 'goodness-of-fit'. Results are given as means ± standard deviation, unless otherwise indicated. For amplitude histograms with distinct peaks, the maximum likelihood solution of the sum of Gaussians was compared with that of unimodal models fitted to the experimental distribution using the expectation–maximization algorithm (Kullmann, 1989; Stricker, Redman & Daley, 1994). For each comparison, the best-fitting unimodal model, as the null hypothesis (H_0), was tested against the alternative (H_1) best-fitting sum of Gaussians. As a test statistic, we used the log-likelihood ratio (Wilks statistic; Wilks, 1938). The significance level for rejection was obtained by comparing the actual log-likelihood ratio with a log-likelihood ratio distribution estimated by fitting the two competing models to each of 300 Monte Carlo samples from the unimodal model (H_0; Stricker *et al.* 1994). We also applied a non-parametric bootstrap test for multimodality (Silverman, 1981; Efron & Tibshirani, 1993). In this test, 1000 bootstrap samples were made from a smooth unimodal estimate of the experimental distribution. This estimate was the Gaussian kernel density estimate which used the least amount of smoothing among all Gaussian kernel density estimates with one mode, i.e. it was the density estimate closest to our data that was consistent with one mode. This estimate was rescaled to have its variance equal to the sample variance. For each bootstrap sample the critical amount of smoothing necessary in order to produce a density estimate with only one mode was determined. If the critical amount of smoothing for the experimental distribution consistently exceeded that of the bootstrap samples, then the hypothesis that the underlying distribution is unimodal was rejected (Silverman, 1981).

RESULTS

Spontaneous fast EPSCs were recorded from twenty-six neurones of the dLGN in the presence of $GABA_A$ (100 μM picrotoxin or 20 μM bicuculline methochloride) and NMDA (50 μM APV) receptor blockers (Fig. 1*A* and *B*). The amplitude, rise time and fall time of all spontaneous EPSCs detected during selected epochs of 1–10 min with stable access resistance (< 10% change) were measured for each neurone. The number of events recorded during an epoch ranged from 116 to 1635 with a mean of 545 events. An amplitude frequency histogram was plotted for each epoch. In eight cells, kinetic properties of spontaneous EPSCs were compared with those of EPSCs evoked by stimulation of putative single retinal input fibres (Paulsen & Heggelund, 1994).

Spontaneous EPSCs with a waveform similar to EPSCs evoked by stimulation of retinal afferents were observed in all cells. The events had a rise time of less than 1 ms (Paulsen & Heggelund, 1994). The spontaneous EPSCs were resistant to bath application of 1 μM tetrodotoxin ($n = 5$; Fig. 1*A*), reversed around 0 mV and were reversibly blocked by bath application of 10 μM CNQX ($n = 6$) as previously demonstrated for evoked EPSCs (Paulsen & Heggelund, 1994). They were therefore regarded as miniature EPSCs mediated by non-NMDA glutamate receptors. In a few cells we occasionally noticed spontaneous events with very small amplitudes and a rise time of several milliseconds. Since the waveform differed clearly from the waveform of events evoked from the optic tract these events were assumed to arise from a different set of synapses, presumably from non-retinal input at more distal locations of the dendritic tree. They were therefore not included in the material presented below.

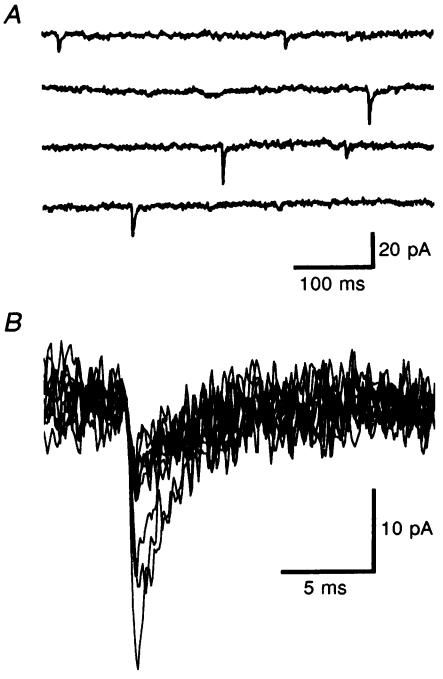

Figure 1. Spontaneous EPSCs from a neurone of the dLGN
The recordings were made in the presence of 100 μM picrotoxin and 50 μM APV at a holding potential of −68 mV. *A*, representative traces. The upper two traces are from the control condition; the lower two traces were obtained in the presence of 1 μM tetrodotoxin. *B*, ten superimposed traces at a higher resolution recorded in the presence of 1 μM tetrodotoxin and aligned at the start of each spontaneous EPSC.

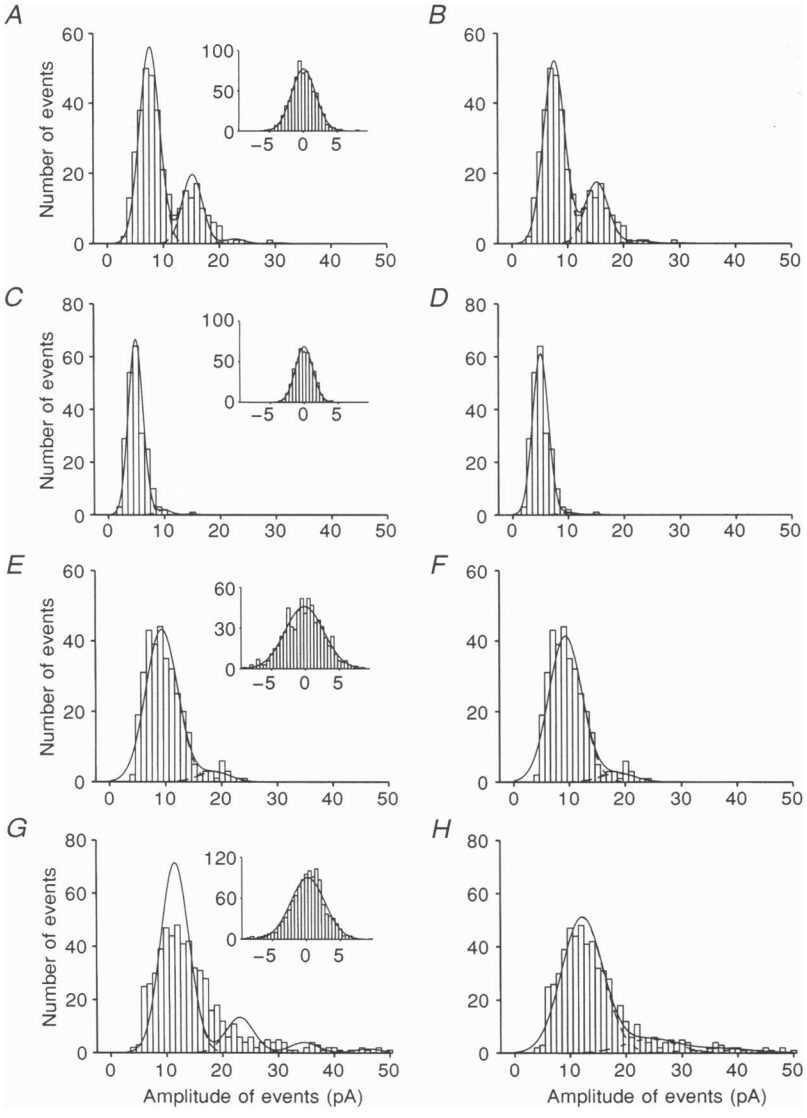

Figure 2. Representative amplitude histograms of spontaneous EPSCs from four cells, demonstrating different proportions of putative multiquantal events

A sum of Gaussian distributions with equidistant means and variance equal to the noise variance has been fitted to each data set with the maximum likelihood method, and is superimposed on each histogram to the left (*A*, *C*, *E* and *G*). The noise distribution is shown as an inset to the upper right of each of these histograms. The mean of the first Gaussian: *A*, 7·6 pA; *C*, 5·0 pA; *E*, 9·3 pA; and *G*, 11·5 pA. The standard deviation of the noise: *A*, 1·8 pA; *C*, 1·3 pA; *E*, 2·9 pA; and *G*, 2·6 pA. The fit for the cell in *G* was rejected with the Kolmogorov–Smirnov goodness-of-fit test ($P < 0·05$) but the fits for cells in *A*, *C* and *E* were not (*P* values of 0·68, 0·49 and 0·16, respectively). To the right (*B*, *D*, *F* and *H*), a sum of Gaussian distributions has been fitted, with means equal to integer multiples of an amplitude close to the modal value and variances equal to the sum of the noise variance and an additional non-negative variance term increasing linearly with successive peaks. The mean of the first Gaussian: *B*, 7·6 pA; *D*, 5·0 pA; *F*, 9·4 pA; and *H*, 12·2 pA. The estimated variance in addition to the noise variance corresponds to a quantal coefficient of variation of: *B*, 0·10; *D*, 0·12; *F*, 0·10; and *H*, 0·23. K–S tests for goodness-of-fit gave the following *P* values: *B*, 0·63; *D*, 0·65; *F*, 0·24; and *H*, 0·43. Bin size, 1 pA; bin size for noise distribution, 0·5 pA. The data in *A* and *B* are from the same cell as used for Figs 2 and 3 in Paulsen & Heggelund (1994). The number of EPSCs analysed in each cell was 346 (*A* and *B*), 222 (*C* and *D*), 329 (*E* and *F*) and 570 (*G* and *H*).

Amplitude distribution of spontaneous EPSCs

The amplitude of the spontaneous EPSCs for a given cell varied over a large range as illustrated by Fig. 2. A considerable part of the variation could be attributed to background noise. The background noise was approximately Gaussian (Fig. 2, insets) with a standard deviation that varied between recorded epochs from 1·2 to 2·9 pA. The average standard deviation of the background noise for all epochs was 2·1 pA. If all the variations were due to noise, and the true amplitudes of all spontaneous events were the same, the amplitude histogram should have been a single Gaussian with mean equal to the quantal size. This was not the case. In all cells the amplitude histograms were skewed towards larger amplitudes and significantly different from a single Gaussian distribution with mean equal to the modal value and standard deviation equal to the standard deviation of the noise distribution ($P < 0{\cdot}05$; K–S test). Most histograms could, however, be adequately fitted by a sum of Gaussians with means equal to integer multiples of the modal value (Fig. 2), suggesting that spontaneous EPSCs with larger amplitudes may represent multiquantal events.

The multiquantal characteristic was most clearly demonstrated in four cells that had prominent peaks in the amplitude histogram with peak separation approximately corresponding to the modal value. An example from one of these cells is shown in Fig. 2*A*. The multimodal amplitude distributions for these cells were not artifactually generated by a particular choice of bins in the histograms, since different bin widths and different centring of the bins did not appreciably change the form or modal values of the histograms. Neither could time-dependent changes explain the result, because the peak positions remained the same in histograms made from different time windows within the same epoch. These histograms therefore suggest that the amplitude of the spontaneous EPSCs was quantally distributed with the modal value as the quantal size (Paulsen & Heggelund, 1994).

In the majority of cells the multimodality of the histograms was less pronounced. In two cells most of the distribution could be accounted for by a single quantum convolved with the amplitude distribution of the background noise (Fig. 2*C*). The majority of cells had more events of larger amplitude than these two cells, and a shape of the amplitude histogram between those illustrated in Fig. 2*A* and *C* as shown in Fig. 2*E*. Four cells had amplitude histograms that were highly skewed towards larger amplitudes but without pronounced, regularly spaced peaks (Fig. 2*G*).

In several histograms the first peak approximated a normal distribution, and the width of the distribution seemed to be close to the width of the noise distribution for the actual epoch (Fig. 2*A*, *C* and *E*). As a first approximation we therefore tested the hypothesis that the amplitude distributions were composed of a sum of Gaussians with mean values equal to integer multiples of an amplitude close to the modal value of the composite histogram, and a standard deviation equal to the standard deviation of the background noise. The model was fitted to the data by the maximum likelihood method (Kullmann, 1989). In this way the curve fitting was independent of the binning of the histograms. The histograms for fourteen of the cells could be accounted for by this model ($P > 0{\cdot}05$, mean P values for these cells, 0·29; K–S test). Examples are shown in Fig. 2*A*, *C* and *E*. This result suggested that in these cells there was little variance in addition to the noise variance. For the rest of the cells this simple model was rejected ($P < 0{\cdot}05$, K–S test; Fig. 2*G*).

By removing the constraint that the variance should be equal to the noise variance, better fits were obtained for most cells by increasing the variance of the Gaussians. This suggested that there was a measurable biological quantal variance in addition to the background noise. A quantal model incorporating quantal variance was therefore fitted to each histogram. A sum of Gaussians was fitted by maximum likelihood estimation (Fig. 2*B*, *D*, *F* and *H*). The means of the Gaussians increased with a constant step size that corresponded to an amplitude close to the modal value of the amplitude histogram. The variance of each Gaussian was equal to the sum of the noise variance and an additional non-negative variance term. This additional term increased linearly with the number of the Gaussian in the series. The K–S goodness-of-fit test was passed for twenty-four of the twenty-six cells ($P > 0{\cdot}05$; mean $P = 0{\cdot}45$).

For the fits passing the K–S test the quantal size was estimated as the mean of the first Gaussian. The quantal variance was estimated as the additional variance for the first Gaussian that had to be added to the noise variance to optimize the fit of the quantal model. The estimated quantal size for these cells ranged from 84 to 225 pS, with a mean of 152 ± 37 pS. The estimated quantal coefficient of variation ranged from 1 to 23% with a mean of 15%. The fraction of events contained in the first Gaussian varied between cells from 62 to 98% with a mean of 88%. The fraction of putative single quanta, double quanta, triple quanta, and four or more quanta for all these cells is shown in Fig. 3.

For several cells the number of detected events with very small amplitudes was below the number predicted from the maximum likelihood solution. This may be due to a failure to distinguish the smallest events from background noise.

Amplitude characteristics during application of tetrodotoxin

For seven cells we recorded spontaneous EPSCs in the presence of 1 μM tetrodotoxin. The amplitude histograms under this condition had the same multimodal properties as the histograms recorded without tetrodotoxin. An example of histograms demonstrating multimodal amplitude distribution in the presence of tetrodotoxin is shown in Fig. 4*A* and *B*.

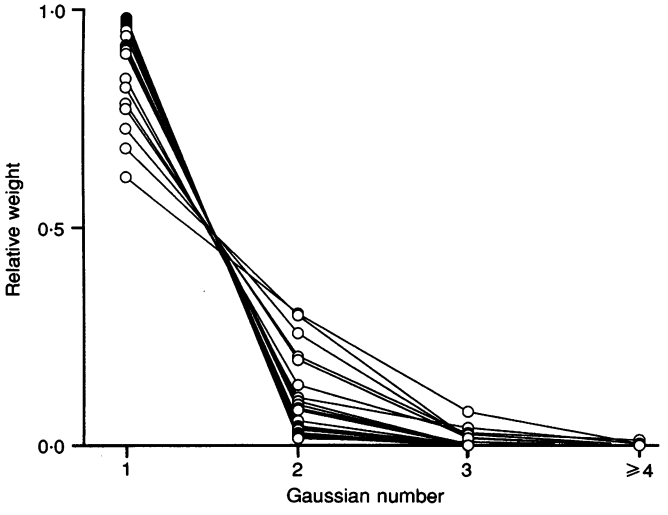

Figure 3. Proportion of events contained in each Gaussian for the quantal model fitted by the maximum likelihood method for cells passing the K–S goodness-of-fit test criterion ($P > 0{\cdot}05$)

The relative weight of each Gaussian is plotted against the Gaussian number as indicated along the abscissa.

For five cells quantal parameters were estimated before and after addition of 1 μM tetrodotoxin. Effective block of Na^+ channels was ensured by demonstrating block of evoked EPSCs ($n = 3$) or block of a fast inward conductance elicited by depolarizing voltage steps ($n = 2$). Addition of tetrodotoxin did not significantly alter any of the quantal parameters estimated by the maximum likelihood method. Thus, the mean estimated quantal parameters before and during application of tetrodotoxin for these five cells were: quantal size, 153 and 152 pS; quantal coefficient of variation, 18 and 21%; and the fraction of events contained in the first Gaussian, 80 and 82%, respectively. The similarity between the quantal parameters obtained before and after application of tetrodotoxin implies that there was no spontaneous impulse activity in the glutamatergic input to the cells. This is reasonable because the excitatory input fibres were transected during slicing of the tissue.

Cells with atypical amplitude histograms

The maximum likelihood solution for the quantal model was rejected in two cells ($P < 0{\cdot}05$; K–S test). One of these is shown in Fig. 5*A*. In these two cells, the maximum likelihood solution gave an estimated quantal size among the three largest in the whole sample. We therefore tentatively hypothesized that the most frequent event in these cells did not correspond to a single quantum, but to a double quantum. On this assumption, good fits of the maximum likelihood solution for the quantal model ($P > 0{\cdot}5$; K–S test) were obtained, as illustrated by Fig. 5*B*, suggesting that spontaneous release of single quanta were virtually lacking in these two cells.

Inadequacy of unimodal models

Although the multiquantal model fitted our data well, we considered the possibility that the peaks in the histograms

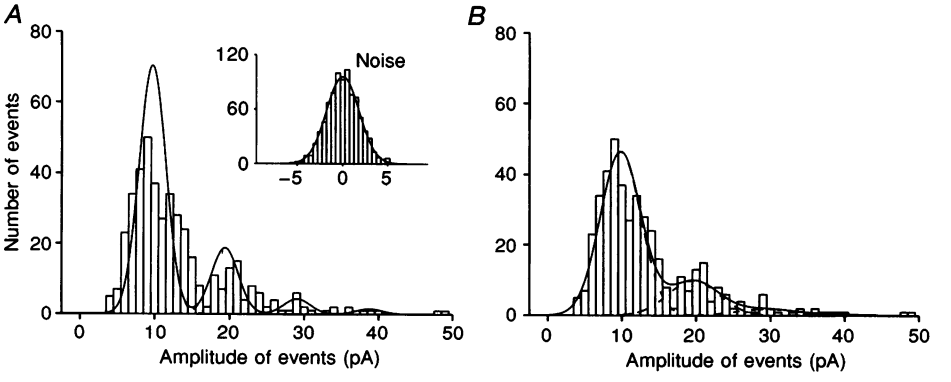

Figure 4. Amplitude histogram of spontaneous EPSCs recorded in the presence of 1 μM tetrodotoxin for one cell

A, the data have been fitted by a sum of Gaussians with variance equal to the noise variance; mean of first Gaussian, 9·7 pA; standard deviation of the noise (inset), 1·8 pA. *B*, the data have been fitted by a quantal model as described in Fig. 2; mean of first Gaussian, 9·8 pA; putative quantal coefficient of variation, 0·21; goodness-of-fit, $P = 0{\cdot}26$ (K–S test). The number of EPSCs analysed was 432. Example traces from the epoch analysed are illustrated in Fig. 1*B*.

might have arisen due to incomplete sampling from an underlying smooth unimodal distribution. Some of the cells could be accounted for by a skewed unimodal model as well as the sum of Gaussians (e.g. the histogram in Fig. 2*G* and *H*). Other cells could be accounted for only by a multimodal model (e.g. the histogram in Fig. 2*A* and *B*). We tested in detail those four cells that had the most prominent peaks, including one cell in the presence of tetrodotoxin (the cell illustrated in Fig. 4*A* and *B*). For these four cells, the maximum likelihood solution of the sum of Gaussians was compared with each of three unimodal models fitted to the experimental distribution by the maximum likelihood criterion. These unimodal models were: a single Gaussian distribution (Clements, 1991), a gamma distribution (McLachlan, 1978), and a cubic transform of a normal random variable (Bekkers *et al.* 1990). For each comparison, we tested whether the best-fitting unimodal model, as the null hypothesis (H_0), could be rejected against the alternative (H_1) quantal model with quantal variance. In all four cells, each of the unimodal models was rejected ($P < 0{\cdot}01$; Wilks statistic). Thus, none of these three unimodal models could account for the data in these four cells.

In order to avoid unnecessary assumptions about the underlying distribution when testing for peakiness, we also applied a Silverman test for multimodality (Silverman, 1981; Efron & Tibshirani, 1993), modified to test whether the second peak might arise by chance due to incomplete sampling from an underlying smooth unimodal distribution. In order to avoid spurious peaks during the testing, two procedures were used. Either, the experimental sample was truncated at an amplitude 2·5 times the modal value, and the test applied on this sample, or, when applying the test for the whole sample, modes were counted only in a window with an upper limit equal to 2·5 times the modal value. With both procedures and for all four cells, the hypothesis that there was only one mode in the underlying distribution was rejected ($P < 0{\cdot}05$, Silverman test). Thus, whereas the multiquantal model could account for all our data, the unimodal models failed to do so. Therefore, to account for spontaneous EPSCs in all cells, the multiquantal model seemed to be the most parsimonious choice.

Kinetic properties of the spontaneous EPSCs

The quantal interpretation of the multimodal amplitude histograms relied on the assumption that the events appearing as unit and double size at the putative somatic recording site reflected single and double quanta at the synaptic sites. Alternatively, the different steps of amplitude we recorded could reflect spontaneous events of similar amplitude at the respective synaptic sites, but with the synaptic sites located at stepwise different electrotonic distances from the recording site. If differences in electrotonic distances were to account for the differences in amplitudes, the rise time of the events should be faster with increasing amplitude of the events (e.g. Spruston, Jaffe, Williams & Johnston, 1993). To test this hypothesis, we compared the waveform of synaptic events of different amplitudes. First, we compared in eight cells the waveform of an average of a number of spontaneous events with that of events evoked by single-pulse electrical stimulation in the optic tract (Paulsen & Heggelund, 1994). In all these cells, the averaged waveform of spontaneous events was similar to that of evoked events when scaled to the same peak amplitude. This suggested that the spontaneous events originated from sites at about the same electrotonic distance as evoked events, consistent with the hypothesis that the spontaneous EPSCs we studied were generated at the synapses receiving retinal input. The waveform of the

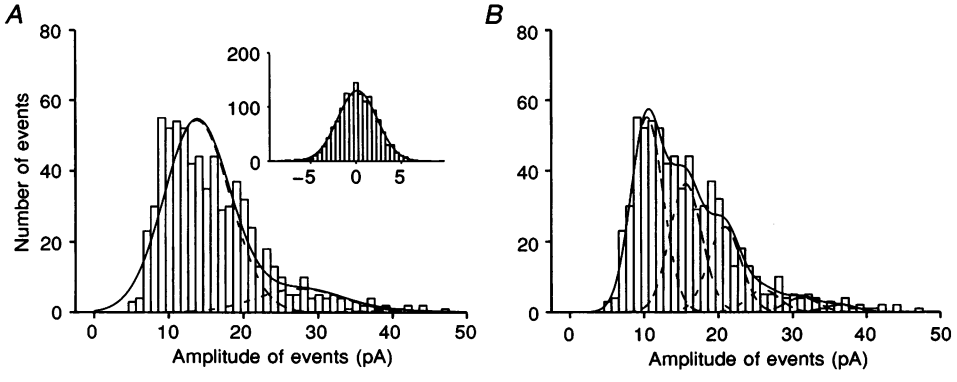

Figure 5. Atypical amplitude histogram

The histogram is made from 707 spontaneous EPSCs recorded in one of two cells for which the simple quantal model was rejected. *A*, maximum likelihood estimate for a sum of Gaussians with equidistance close to the modal value. Equidistance, 13·8 pA; standard deviation of the noise, 2·2 pA; quantal coefficient of variation, 0·28. This fit was rejected ($P < 0{\cdot}05$, K–S test). *B*, maximum likelihood estimate for a sum of Gaussians with twice the equidistance close to the modal value. Equidistance, 5·2 pA; quantal coefficient of variation, 0·03; goodness-of-fit, $P = 0{\cdot}91$ (K–S test).

spontaneous events was the same during application of tetrodotoxin. An example is shown in Fig. 6*A*. The upper trace shows the average of spontaneous EPSCs recorded before tetrodotoxin application. The lower trace shows the average of miniature EPSCs recorded during application of tetrodotoxin. In both cases the average trace is compared with an average trace of the evoked EPSC scaled to the same peak amplitude (smooth trace). Next, we compared averages of spontaneous events taken from the various Gaussians. The average traces were obtained by alignment of single traces on the start of the rising phase of the current. Overall, the waveform looked similar for small and large events, when scaled to the same peak amplitude. In no cell did we observe faster rise times with increasing amplitude. This is evidence against the hypothesis that differences in electrotonic distance from the recording site might account for the differences in amplitude. It indicates that the events included in the various Gaussians may rather be generated at similar electrotonic distances from the recording site, and that they reflect genuine steps in EPSC amplitude at the synaptic sites.

Although the waveform of the events corresponding to the various Gaussians was similar, a tendency for the rise time to become slower with larger amplitudes was noted. An example is shown in Fig. 6*B*. To analyse this further, the rise time of each event was plotted against the absolute value of the peak amplitude of the event. This was done for each cell. The plots showed a slight increase in rise time with increasing peak amplitude. This was expressed as a weak-to-moderate positive correlation between the absolute value of the peak amplitude and rise time in all cells. The average correlation coefficient for all cells was 0·45. A positive correlation is the opposite of that expected if differences in electrotonic distance were to account for the variation in amplitude of EPSCs. By linear regression, the rise time was estimated to increase by 16 ± 8 μs for every 1 pA increase of peak amplitude. Figure 6*C* shows a scatter plot of rise time *versus* peak amplitude with a moderate correlation. A similar analysis has been made on simulated data by Ankri, Legendre, Faber & Korn (1994).

In order to see if the quantal distribution of the amplitudes was accompanied by similar subpopulations of rise time, 2-dimensional kernel density estimation was carried out (Sheather & Jones, 1991; Venables & Ripley, 1994). An example obtained in the presence of tetrodotoxin is shown in Fig. 7. The diagram shows distinct subpopulations along the amplitude axis, whereas such subpopulations were not evident along the axis of rise time. This is consistent with the hypothesis that the events originate from the same population of synapses.

The mean rise time for the spontaneous events varied between cells from 0·3 to 0·6 ms. The mean rise time for all cells was 0·4 ± 0·09 ms. The mean fall time varied between cells from 1·3 to 3·4 ms. The mean fall time for all cells was 2·3 ± 0·5 ms. Only a weak positive correlation was found between peak amplitude of the events and the fall time. The mean correlation coefficient for all cells was 0·23.

Frequency of spontaneous EPSCs

The mean frequency of detected spontaneous EPSCs varied between cells from 0·7 to 6·3 Hz with a mean of 3·1 ± 1·7 Hz. One outlier, which was excluded from the estimate of the mean, had a frequency of 17·7 Hz.

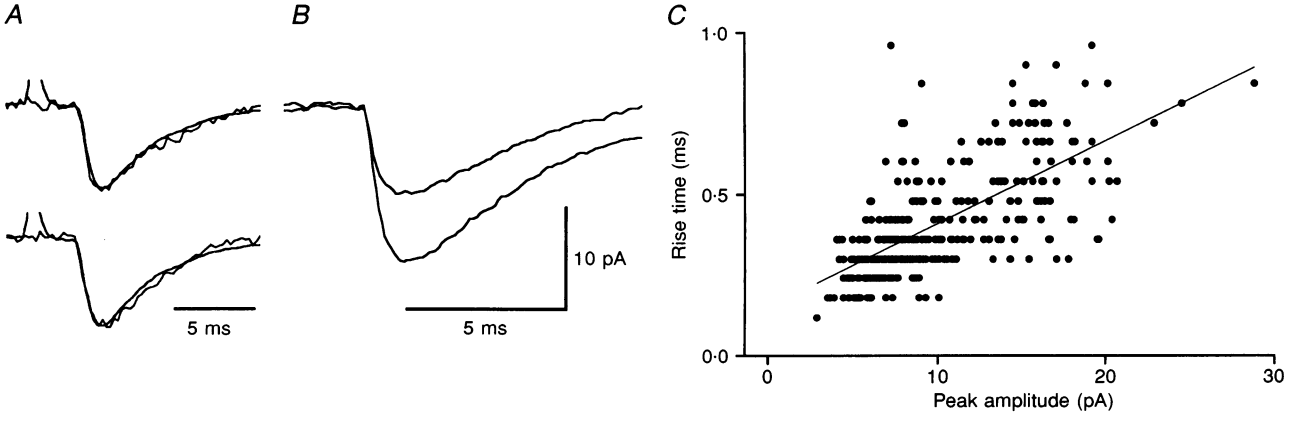

Figure 6. Kinetic properties of spontaneous EPSCs

The data are from the same cell as illustrated in Fig. 2*A* and *B*. *A*, mean of 20 spontaneous EPSCs aligned at the start of the EPSC superimposed on the mean of 8 evoked EPSCs. The relative scale was 1 : 12. Upper traces, spontaneous EPSCs recorded in control condition. Lower traces, spontaneous EPSCs recorded in 1 μM tetrodotoxin. *B*, mean of 74 spontaneous EPSCs from the second Gaussian aligned at the start of each EPSC superimposed on a corresponding mean of EPSCs with amplitudes centred around the mean of the first Gaussian. Traces contaminated by other spontaneous events were excluded from the calculation of these mean traces. *C*, scatter plot of rise time *versus* peak amplitude for all detected events for this cell. The regression line is drawn. The correlation coefficient for rise time and peak amplitude for this cell was 0·67.

To determine whether the spontaneous events occurred independently of each other, inter-event interval histograms were made. If the sequence of events was completely irregular, the inter-event histograms should be exponential and fit the graph of the probability density for intervals between successive events given by:

$$n = (N\Delta t)re^{-rt}, \quad (1)$$

where n is the number of intervals in a given histogram bin with a bin width of Δt seconds, N is the total number of intervals in the histogram, r is the average rate of events (events s^{-1}), and t is the interval (Fatt & Katz, 1952; Johnston & Wu, 1995).

The inter-event interval histograms were approximately exponential, as illustrated by the example in Fig. 8*A*. The amplitude histogram for this cell is shown in Fig. 4*A* and *B*. The inter-event interval histogram could be fitted by the exponential probability density function ($P = 0{\cdot}83$, d.f. = 27; χ^2 test), consistent with the idea that the spontaneous EPSCs are independent events. Corresponding results were found for other cells. Adequate fit ($P > 0{\cdot}05$; χ^2 test) of the inter-event interval histogram to the probability density function was obtained for nineteen of the cells.

Possible coupling between quantal release in multiquantal events

Multiquantal events could be caused by summation of randomly occurring spontaneous events of single quantum amplitude. Alternatively, the multiquantal events could reflect coupled, near simultaneous release of several quanta. To investigate these hypotheses we calculated the proportion of the putative double quanta and triple quanta that could be accounted for by summation of randomly occurring events. The time resolution of our recording traces was 0·1 ms (A/D conversion rate), and all the EPSCs had a 20–80% rise time of less than 1 ms. The smallest interval between events that we could resolve was therefore in the range between 0·1 and 1 ms. As a conservative estimate we used 1 ms as the smallest inter-event interval that we could detect, Δt. The probability for the occurrence of such small inter-event intervals, and thereby the probability for double quanta by random summation, is approximately $r\Delta t$, where r is the average rate of events (Fatt & Katz, 1952). The probability for two such intervals to follow each other, thus giving a triple quantum, is $(r\Delta t)^2$. The average rate, in these calculations, was determined by assuming that all double quanta were two events with an inter-event interval of 1 ms, all triple quanta, three events with a 1 ms inter-event interval, and so on.

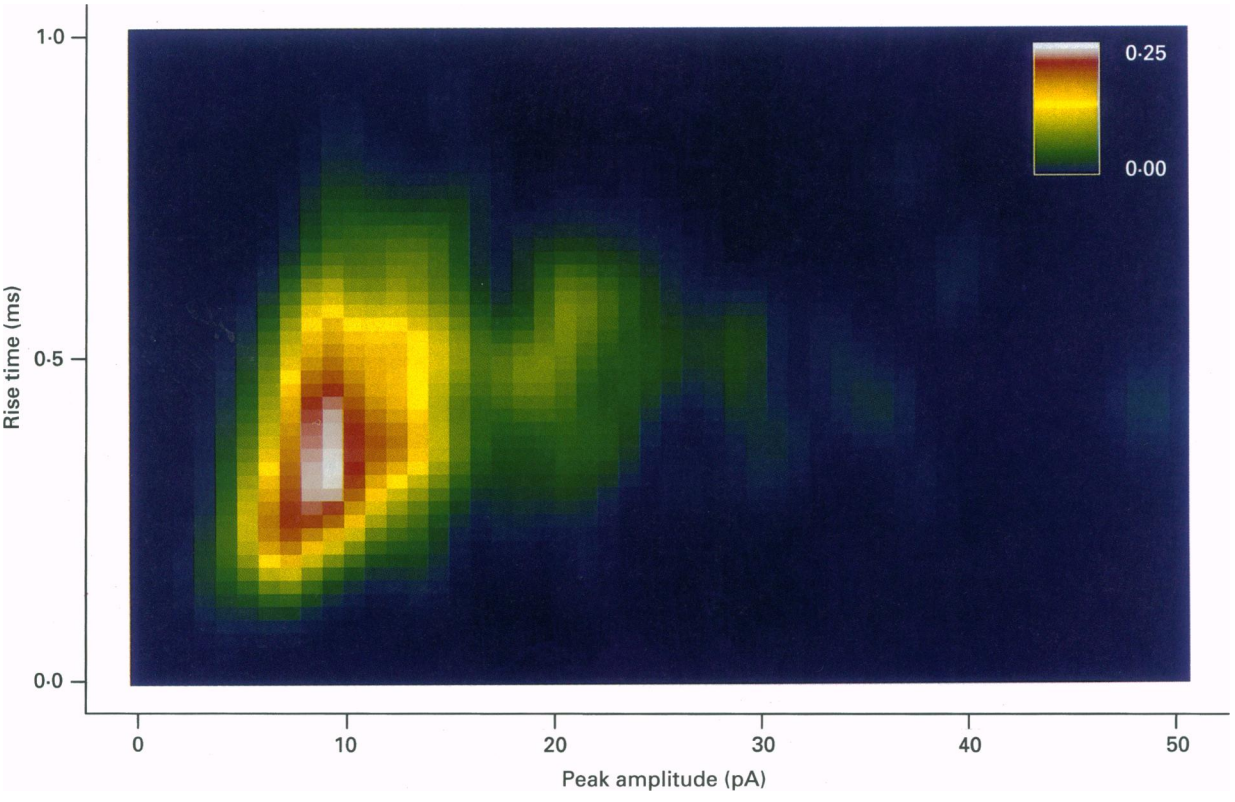

Figure 7. Two-dimensional kernel density plot of rise time *versus* peak amplitude for the cell illustrated in Figs 1, 4*A* and *B*

A Gaussian kernel smoothed the data along each axis. The kernel width was chosen according to Sheather & Jones (1991). The density estimate is colour coded. The colour scale is shown in the upper right part of the diagram. Note distinct clustering of peak amplitudes occurring at regular intervals.

The proportion of double quanta that could be accounted for by random summation varied between cells from 0·003 to 0·150, with a mean of 0·058. The proportion of triple quanta accounted for varied between $< 10^{-12}$ and 0·019, with a mean of 0·0016. For the cell illustrated in Fig. 8 the proportion accounted for was 0·048 for putative double quanta, and 0·0007 for putative triple quanta. Accordingly, the vast majority of the putative multiquantal events may be regarded as genuinely multiquantal, consistent with the hypothesis that there is a coupling of release during the multiquantal events that gives almost simultaneous release of several quanta.

On the assumption that all multiquantal events consisted of single quanta with an inter-event interval of 1 ms, we repeated the test for independence in the occurrence of the events. New inter-event interval histograms were made. For each histogram a new exponential function was calculated by eqn (1). The results showed that the number of 1 ms intervals markedly exceeded the number predicted for a random sequence (Fig. 8*B*). This confirmed that the multiquantal events could not be accounted for by independently occurring single quanta, and indicated coupled release in the multiquantal events. Another possibility remains to be excluded, however, viz. that the response to the release of a single quantum might vary in a stepwise manner between different release sites.

The putative multiquantal events usually had a smooth rising flank from the start to the maximal amplitude as illustrated in Fig. 6*A*. Thus there was no indication from their waveform that they might be generated by almost simultaneous release of multiple quanta. In some putative multiquantal events from a few of the cells, however, notches could be seen in the rising phase, suggesting that the larger events may indeed be composed of smaller units. Examples are shown in Fig. 8*C*. Interestingly, similar composite events reflecting multiple quantal steps were sometimes observed in evoked EPSCs during low calcium (Paulsen & Heggelund, 1994).

DISCUSSION

The results indicate that spontaneous EPSCs may vary in quantal steps. First, for a subset of the cells the amplitude frequency distribution was clearly multimodal with approximately equidistant peaks. Second, the amplitude distributions for all cells could be adequately fitted by a sum of Gaussians with mean values equal to integer multiples of

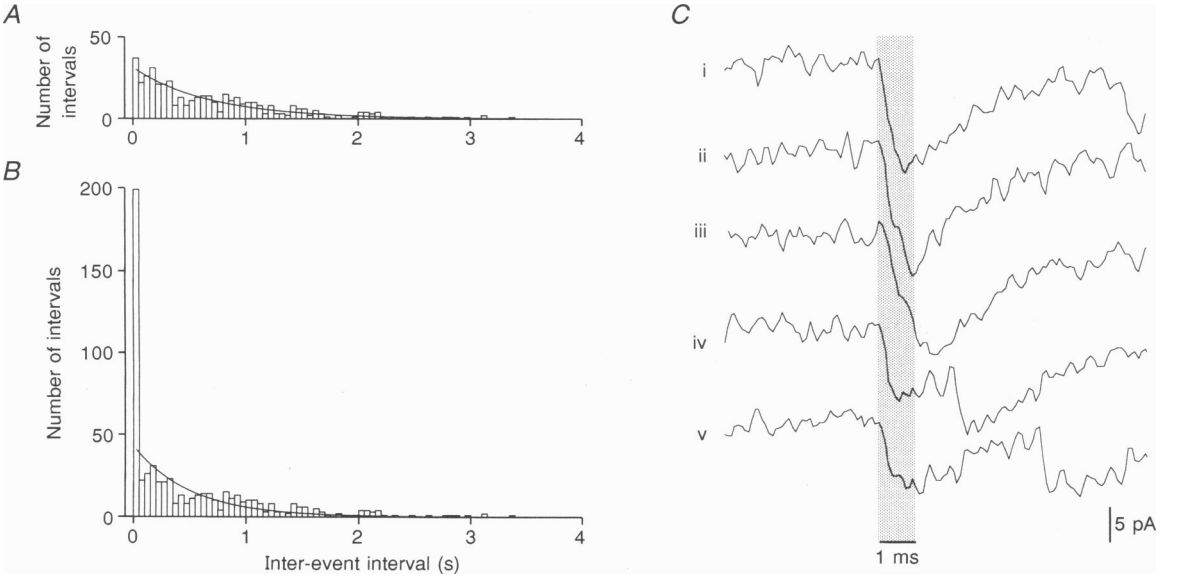

Figure 8. Inter-event interval histograms and single traces for the cell illustrated in Fig. 4*A* and *B*

A, inter-event interval histogram for all spontaneous events ($N = 432$). The smooth curve is an exponential function calculated by eqn (1). The average rate of events was 1·44 s^{-1}. Bin width, 50 ms. *B*, inter-event interval histogram calculated on the assumption that each multiquantal event consisted of single quanta with an inter-event interval of 1 ms. The number of doublets, triplets, etc., were calculated from the proportion of such events given by the weight of the respective Gaussian in the maximum likelihood solution of the quantal model. The exponential curve was calculated by eqn (1). Number of single quanta was 595. Average rate of single quanta was 1·98 s^{-1}. *C*, example traces from the same cell. Traces i–iii, putative double quanta: trace i illustrates an event with a smooth rising phase and an amplitude approximately twice the modal value; traces ii and iii illustrate events with a notch during the rising phase; and traces iv and v illustrate putative single quanta occurring close in time. These events would be measured as two separate spontaneous events. The grey shaded area indicates the slowest rise time for events that would be measured as one spontaneous event during our analysis.

a quantal size, and a variance determined by the measurement noise and a quantal variance factor. For the majority of cells the modal value of the distribution corresponded approximately to the equidistance between the Gaussians indicating that single quanta occurred most frequently in these cells. For a few cells the modal value corresponded approximately to twice the equidistance, suggesting that singlets were infrequent in these cells. The quantal variance was small. The quantal characteristics persisted in tetrodotoxin. The results suggest that the large amplitude variation and the skewed amplitude histogram of spontaneous EPSCs can be accounted for mainly by the occurrence of spontaneous multiquantal events. Accordingly, a spontaneous event may not always reflect a single quantum.

The quantal size was assumed to correspond to the first mode in the amplitude distribution for the majority of cells. One might argue that the first mode could be formed by the sum of two or more distributions of a quantal size considerably smaller than the modal value of our amplitude histograms. This appears to be unlikely for two reasons. First, the amplitude distribution could be adequately fitted by a sum of Gaussians with an equidistance approximately equal to the value of the first mode. Second, for a set of cells where evoked events were recorded under low extracellular calcium, the first mode in the amplitude distribution of both spontaneous and evoked events occurred at about the same value (Paulsen & Heggelund, 1994), and for both distributions this value corresponded to the unit step in evoked events as in the classical estimates of a quantal unit in the neuromuscular junction (del Castillo & Katz, 1954).

An alternative and, in general, a better way to estimate the quantal size, would be to estimate it from the distance between peaks determined by global optimization with numerous initial values and different values of components (Edwards *et al.* 1990). In our material the first peak dominated the amplitude distributions, as illustrated by Fig. 2. Estimation of quantal size from this peak seemed therefore to be a reasonable choice in the present case.

The estimated mean quantal size was 152 pS. This is somewhat higher than the median value of fast spontaneous EPSCs recorded in CA3 neurones (106 pS; Jonas *et al.* 1993). Both estimates are likely to be underestimates of the conductance change at the subsynaptic membrane because of inevitable space and voltage clamp errors. Jonas *et al.* (1993) estimated that the conductance change by the opening of a single non-NMDA receptor-operated channel is 8·5 pS in CA3 pyramidal cells in the hippocampus. Assuming the same single channel conductance in the cells we recorded from, the quantal size in our study would correspond to the opening of only eighteen channels.

The variance of the Gaussian fits revealed a variance in excess of the noise variance. Our estimate of the quantal variance relied on the asumption that the noise variance and quantal variance are independent and add linearly. The estimate we obtained for the quantal coefficient of variation was ~0·15, similar to that estimated for evoked excitatory events in the mossy fibre–CA3 pyramidal cell synapse (~0·22; Jonas *et al.* 1993). The estimate is smaller than the estimate of ~0·30 at the neuromuscular junction (Fatt & Katz, 1952; del Castillo & Katz, 1954; Boyd & Martin, 1956), but larger than estimates extracted with deconvolution techniques from microelectrode recordings in the spinal cord (< 0·05; Jack *et al.* 1981). Still, the expected intrinsic variance of a synaptic junction associated with opening of a small number of receptor channels (Faber, Young, Legendre & Korn, 1992) is sufficient to account for most of the quantal variance in our experiments. The estimate of quantal variance includes variance intrinsic to the synaptic junction as well as variance between synaptic junctions. Our analysis therefore suggests that for the dLGN neurones, both the intrinsic junctional variance and the variance between individual junctions are relatively small.

Problems with detecting events in the smallest amplitude range could have led to an underestimation of the quantal variance in our study. The smallest events had amplitudes within the amplitude range of the background noise. Such events were detectable only when their characteristic waveform was clearly recognized. Several of the smallest events were therefore probably not detected due to distortion by noise. This was indicated by the fact that the amplitude histogram for several cells fell below the lower tail of the maximum-likelihood solution of the quantal model.

Difficulties with the detection of the smallest spontaneous events could also contribute to the positive correlation we found between rise time and amplitude (Ankri *et al.* 1994). This correlation depended to a certain extent on the particularly short rise time of the smallest events (Fig. 6*C*). The sharply rising events of the smallest amplitudes were easier to detect in the noisy traces than more slowly rising events of similar amplitude. Thus, it is reasonable to assume that some of the events with small amplitude and relatively slow rise time were lost in the background noise during the selection of events from the original recording traces. Another factor that might have contributed to the positive correlation between rise time and amplitude is a slight asynchrony of putative components in multiquantal events indicated by the notches in the rising phase in some of the events (Fig. 8*C*).

The quantal properties at the recording site most probably reflected genuine stepwise amplitudes at the synaptic sites because the waveform of spontaneous events of the various amplitudes was similar. The waveform was also similar to the waveform of events evoked by electrical stimulation of the retinal afferents. The amplitude variation of the EPSCs was therefore not caused by differences in electrotonic distance to the electrode from the different synaptic sites. In

fact, the positive correlation we found between peak amplitude and rise time is the opposite of that expected if dendritic cable properties were to explain the amplitude variation. The multiquantal events were most probably also genuinely multiquantal in the sense that they could not be accounted for by summation of randomly occurring spontaneous events of the quantal size. The possibility that the response to a quantal release might vary in a stepwise manner between different release sites was not ruled out, however.

Spontaneous multiquantal events have been reported from a number of different synapses, including the neuromuscular junction (Liley, 1957), synapses in peripheral ganglia (Bornstein, 1978), and central inhibitory synapses (Edwards *et al.* 1990; Ropert *et al.* 1990; Korn, Bausela, Charpier & Faber, 1993). For excitatory synaptic transmission in the mammalian brain it has been difficult to demonstrate multiquantal spontaneous events. Broad amplitude frequency distribution of miniature synaptic currents skewed towards larger amplitudes has been reported from individual excitatory synapses between cultured hippocampal neurones (Bekkers *et al.* 1990). Since no clear peaks in the amplitude distributions were found in that study, all of the variance was attributed to variation of quantal size at each synaptic junction, although multiquantal events were not ruled out. Broad amplitude frequency distributions for spontaneous EPSCs skewed towards larger amplitudes have also been reported for the transmission between mossy fibre terminals and granule cells in cerebellar slices (Silver *et al.* 1992), and between mossy fibre and CA3 pyramidal cells in hippocampal slices (Jonas *et al.* 1993). The problems of demonstrating multiquantal spontaneous events in excitatory synapses in the brain have probably partly been caused by the small magnitude of the quantal size in these synapses compared with background noise, and are partly due to the fact that the synapses in most systems are distributed over a considerable dendritic distance, thereby adding amplitude variability due to cable properties. Miniature EPSCs recorded from motoneurones in organotypic cultures from the spinal cord have been reported to be consistent with a multiquantal model when corrected for dendritic cable properties (Ulrich & Lüscher, 1993). The likelihood of demonstrating multiquantal spontaneous EPSCs in the dLGN cells is good because these cells are electrotonically compact (Bloomfield *et al.* 1987; Crunelli *et al.* 1987), and receive excitatory input from retinal terminals at proximal synapses (Wilson *et al.* 1984; Hamos *et al.* 1987; Robson, 1993). From a combined anatomical and theoretical analysis it was suggested (Hamos *et al.* 1987) that retinogeniculate synapses are located at approximately the same electrotonic distance from the soma. As in other systems the amplitude distributions of the spontaneous EPSCs for dLGN cells were broad and skewed towards larger amplitudes, but we could show that the tail of the distribution could be accounted for mainly by the occurrence of multiquantal events as in other transmitter systems. Therefore, spontaneous multiquantal events may occur also in excitatory, glutamatergic synapses.

A possible structural correlate for spontaneous multiquantal release is suggested by morphological data from the cat dLGN. Rapisardi & Miles (1984) reported several release sites in each retinal terminal from analysis of serial electron micrographic sections through the cat dLGN. Thus, if the retinal terminals are similar in the guinea-pig dLGN, multiquantal release might arise from events such as calcium sparks in terminals with multiple release sites. A correspondence between multiple release sites in each terminal and the presence of multimodal amplitude histograms for miniatures was reported from GABAergic synapses onto dendrites of Mauthner cells in the goldfish (Korn *et al.* 1993), contrasted by unimodal amplitude distribution and single release sites for glycinergic synapses onto the soma of the same cell type (Korn & Faber, 1990).

For two of the cells in our material the Gaussian model had to be fitted to the amplitude histograms on the asumption that the modal value corresponded approximately to the mean amplitude of the double quanta. Very few events in these cells seemed to be single quanta, i.e. amplitude corresponding to the interpeak separation. Similar findings have been reported in other types of synapses. Edwards *et al.* (1990) presented an amplitude distribution for miniature IPSCs from a cell in the dentate gyrus that had very few events with amplitudes corresponding to the peak separation (their Fig. 9*B*). The most frequent amplitudes of the IPSCs were about twice or triple the interpeak separation. According to the hypothesis discussed above, one would predict that among the relevant types of presynaptic boutons in such cases, few boutons have only one release site, and the majority two or more release sites. Alternatively, each release site might release more than one quantum.

The quantum is a term introduced to describe a unit in synaptic transmission (del Castillo & Katz, 1954). Because the spontaneous events in the original report on the neuromuscular junction had an amplitude distribution which could be fitted by a single Gaussian distribution, it was reasonable to suggest that the spontaneous events represent the quantum. The multimodal amplitude distributions of spontaneous excitatory events in dLGN cells suggest a different relationship between spontaneous events and the quantum. The fact that the amplitude distributions of the spontaneous events could be described by a sum of Gaussians with equidistant means makes it reasonable to determine the unit in the spontaneous events by this equidistance. The unit in the spontaneous events corresponded to the equidistance between peaks in amplitude histograms of evoked events for the same cell (Paulsen & Heggelund, 1994), indicating that this unit reflects the quantum of excitatory transmission in the retinogeniculate synapse.

ANKRI, N., LEGENDRE, P., FABER, D. S. & KORN, H. (1994). Automatic detection of spontaneous synaptic responses in central neurons. *Journal of Neuroscience Methods* **52**, 87–100.

BEKKERS, J. M., RICHERSON, G. B. & STEVENS, C. F. (1990). Origin of variability in quantal size in cultured hippocampal neurons and hippocampal slices. *Proceedings of the National Academy of Sciences of the USA* **87**, 5359–5362.

BLANTON, M. G., LO TURCO, J. J. & KRIEGSTEIN, A. R. (1989). Whole cell recording from neurons in slices of reptilian and mammalian cerebral cortex. *Journal of Neuroscience Methods* **30**, 203–210.

BLOOMFIELD, S. A., HAMOS, J. E. & SHERMAN, S. M. (1987). Passive cable properties and morphological correlates of neurones in the lateral geniculate nucleus of the cat. *Journal of Physiology* **383**, 653–692.

BORNSTEIN, J. C. (1978). Spontaneous multiquantal release at synapses in guinea-pig hypogastric ganglia: evidence that release can occur in bursts. *Journal of Physiology* **282**, 375–398.

BOYD, I. A. & MARTIN, A. R. (1956). The end-plate potential in mammalian muscle. *Journal of Physiology* **132**, 74–91.

CLEMENTS, J. (1991). Quantal synaptic transmission? *Nature* **353**, 396.

CRUNELLI, V., LERESCHE, N. & PARNAVELAS, J. G. (1987). Membrane properties of morphologically identified X and Y cells in the lateral geniculate nucleus of the cat *in vitro*. *Journal of Physiology* **390**, 243–256.

DEL CASTILLO, J. & KATZ, B. (1954). Quantal components of the end-plate potential. *Journal of Physiology* **124**, 560–573.

EDWARDS, F. A., KONNERTH, A. & SAKMANN, B. (1990). Quantal analysis of inhibitory synaptic transmission in the dentate gyrus of rat hippocampal slices: a patch-clamp study. *Journal of Physiology* **430**, 213–249.

EFRON, B. & TIBSHIRANI, R. J. (1993). *An Introduction to the Bootstrap*. Chapman & Hall, New York.

FABER, D. S., YOUNG, W. S., LEGENDRE, P. & KORN, H. (1992). Intrinsic quantal variability due to stochastic properties of receptor–transmitter interactions. *Science* **258**, 1494–1498.

FATT, P. & KATZ, B. (1952). Spontaneous subthreshold activity at motor nerve endings. *Journal of Physiology* **117**, 109–128.

HAMOS, J. E., VAN HORN, S. C., RACZKOWSKI, D. & SHERMAN, S. M. (1987). Synaptic circuits involving an individual retinogeniculate axon in the cat. *Journal of Comparative Neurology* **259**, 165–192.

JACK, J. J. B., REDMAN, S. J. & WONG, K. (1981). The components of synaptic potentials evoked in cat spinal motoneurones by impulses in single group Ia afferents. *Journal of Physiology* **321**, 65–96.

JOHNSTON, D. & WU, S. M.-S. (1995). *Foundations of Cellular Neurophysiology*. MIT Press, Cambridge, MA, USA.

JONAS, P., MAJOR, G. & SAKMANN, B. (1993). Quantal components of unitary EPSCs at the mossy fibre synapse on CA3 pyramidal cells of rat hippocampus. *Journal of Physiology* **472**, 615–663.

KORN, H., BAUSELA, F., CHARPIER, S. & FABER, D. S. (1993). Synaptic noise and multiquantal release at dendritic synapses. *Journal of Neurophysiology* **70**, 1249–1254.

KORN, H. & FABER, D. S. (1990). Transmission at a central inhibitory synapse IV. Quantal structure of synaptic noise. *Journal of Neurophysiology* **63**, 198–222.

KULLMANN, D. M. (1989). Applications of the expectation-maximization algorithm to quantal analysis of postsynaptic potentials. *Journal of Neuroscience Methods* **30**, 231–245.

KULLMANN, D. M. & NICOLL, R. A. (1992). Long-term potentiation is associated with increases in quantal content and quantal amplitude. *Nature* **357**, 240–244.

LARKMAN, A., STRATFORD, K. & JACK, J. (1991). Quantal analysis of excitatory synaptic action and depression in hippocampal slices. *Nature* **350**, 344–347.

LIAO, D., JONES, A. & MALINOW, R. (1992). Direct measurement of quantal changes underlying long-term potentiation in CA1 hippocampus. *Neuron* **9**, 1089–1097.

LILEY, A. W. (1957). Spontaneous release of transmitter substance in multiquantal units. *Journal of Physiology* **136**, 595–605.

MCLACHLAN, E. M. (1978). The statistics of transmitter release at chemical synapses. *International Review of Physiology: Neurophysiology* III **17**, 49–117.

PAULSEN, O. & HEGGELUND, P. (1994). The quantal size at retinogeniculate synapses determined from spontaneous and evoked EPSCs in guinea-pig thalamic slices. *Journal of Physiology* **480**, 505–511.

RAASTAD, M., STORM, J. F. & ANDERSEN, P. (1992). Putative single quantum and single fibre excitatory postsynaptic currents show similar amplitude range and variability in rat hippocampal slices. *European Journal of Neuroscience* **4**, 113–117.

RAPISARDI, S. C. & MILES, T. P. (1984). Synaptology of retinal terminals in the dorsal lateral geniculate nucleus of the cat. *Journal of Comparative Neurology* **223**, 515–534.

REDMAN, S. (1990). Quantal analysis of synaptic potentials in neurons of the central nervous system. *Physiological Reviews* **70**, 165–198.

ROBSON, J. A. (1993). Qualitative and quantitative analyses of the patterns of retinal input to neurons in the dorsal lateral geniculate nucelus of the cat. *Journal of Comparative Neurology* **334**, 324–336.

ROPERT, N., MILES, R. & KORN, H. (1990). Characteristics of miniature inhibitory postsynaptic currents in CA1 pyramidal neurones of rat hippocampus. *Journal of Physiology* **428**, 707–722.

SHEATHER, S. J. & JONES, M. C. (1991). A reliable data-based bandwidth selection method for kernel density estimation. *Journal of the Royal Statistical Society* B **53**, 683–690.

SILVER, R. A., TRAYNELIS, S. F. & CULL-CANDY, S. G. (1992). Rapid-time-course miniature and evoked excitatory currents at cerebellar synapses *in situ*. *Nature* **355**, 163–166.

SILVERMAN, B. W. (1981). Using kernel density estimates to investigate multimodality. *Journal of the Royal Statistical Society* B **43**, 97–99.

SPRUSTON, N., JAFFE, D. B., WILLIAMS, S. H. & JOHNSTON, D. (1993). Voltage- and space-clamp errors associated with the measurement of electrotonically remote synaptic events. *Journal of Neurophysiology* **70**, 781–802.

STERN, P., EDWARDS, F. A. & SAKMANN, B. (1992). Fast and slow components of unitary EPSCs on stellate cells elicited by focal stimulation in slices of rat visual cortex. *Journal of Physiology* **449**, 247–278.

STRICKER, C., REDMAN, S. & DALEY, D. (1994). Statistical analysis of synaptic transmission: model discrimination and confidence limits. *Biophysical Journal* **67**, 532–547.

ULRICH, D. & LÜSCHER, H.-R. (1993). Miniature excitatory synaptic currents corrected for dendritic cable properties reveal quantal size and variance. *Journal of Neurophysiology* **69**, 1769–1773.

VAN DER KLOOT, W. (1991). The regulation of quantal size. *Progress in Neurobiology* **36**, 93–130.

VENABLES, W. N. & RIPLEY, B. D. (1994). *Modern Applied Statistics with S-Plus*. Springer-Verlag, New York.

WILKS, S. S. (1938). The large-sample distribution of the likelihood ratio for testing composite hypotheses. *Annals of Mathematical Statistics* **9**, 60–62.

WILSON, J. R, FRIEDLANDER, M. J. & SHERMAN, S. M. (1984). Fine structural morphology of identified X- and Y-cells in the cat's lateral geniculate nucleus. *Proceedings of the Royal Society* B **221**, 411–436.

Acknowledgements

We wish to thank Drs Angelo Canty and Anthony C. Davison in the Department of Statistics, Oxford, for advice and for sharing a bootstrap function for use with S-Plus. We are grateful to Drs Dimitri Kullmann and Christian Stricker for kindly sharing their software for maximum likelihood estimation (Kullmann, 1989, and Stricker *et al.* 1994). Mr Bruce Piercy, Mr Lucas G.W.D. Scholte and Mr M. Mobyholt are thanked for programming assistance. The project was financially supported by The Research Council of Norway, and the Nansen Foundation. O.P. is the Christopher Welch Junior Research Fellow at Wadham College, Oxford.

Author's email address

P. Heggelund: paul.heggelund@basalmed.uio.no

Received 20 December 1995; accepted 11 July 1996.